Mon. Not. R. Astron. Soc. **383,** 1359–1365 (2008) doi:10.1111/j.1365-2966.2007.12659.x

Cosmic ray confinement in fossil cluster bubbles

M. Ruszkowski,[1,2⋆] T. A. Enßlin,[2] M. Brüggen,[3] M. C. Begelman[4,5] and E. Churazov[2,6]

[1]*Department of Astronomy, The University of Michigan, 500 Church Street, Ann Arbor, MI 48109, USA*
[2]*Max Planck Institute for Astrophysics, Karl-Schwarzschild-Str. 1, 85741 Garching, Germany*
[3]*Jacobs University Bremen, Campus Ring 1, 28759 Bremen, Germany*
[4]*JILA, University of Colorado at Boulder, CO 80309-0440, USA*
[5]*Department of Astrophysical and Planetary Sciences, University of Colorado, Boulder, CO 80309-0391, USA*
[6]*Space Research Institute, Profsoyuznaya Str. 84/32, Moscow 117997, Russia*

Accepted 2007 November 1. Received 2007 October 15; in original form 2007 May 23

ABSTRACT

Most cool core clusters of galaxies possess active galactic nuclei (AGN) in their centres. These AGN inflate buoyant bubbles containing non-thermal radio-emitting particles. If such bubbles efficiently confine cosmic rays (CRs) then this could explain 'radio relics' seen far from cluster centres. We simulate the diffusion of CRs from buoyant bubbles inflated by AGN. Our simulations include the effects of the anisotropic particle diffusion introduced by magnetic fields. Our models are consistent with the X-ray morphology of AGN bubbles, with disruption being suppressed by the magnetic draping effect. We conclude that for such magnetic field topologies, a substantial fraction of CRs can be confined inside the bubbles on buoyant rise time-scales even when the parallel diffusivity coefficient is very large. For isotropic diffusion at a comparable level, CRs would leak out of the bubbles too rapidly to be consistent with radio observations. Thus, the long confinement times associated with the magnetic suppression of CRs diffusion can explain the presence of radio relics. We show that the partial escape of CRs is mostly confined to the wake of the rising bubbles and speculate that this effect could: (i) account for the excitation of the Hα filaments trailing behind the bubbles in the Perseus cluster, (ii) inject entropy into the metal-enriched material being lifted by the bubbles and, thus, help to displace it permanently from the cluster centre and (iii) produce observable γ-rays via the interaction of the diffusing CRs with the thermal intracluster medium.

Key words: magnetic fields – MHD – cosmic rays.

1 INTRODUCTION

The discovery of X-ray cavities in the intracluster medium (ICM) that coincide with radio emission (e.g. Blanton et al. 2003; Böhringer et al. 2004), sound waves and weak shocks (Fabian et al. 2003a) provided clear observational support for the idea that active galactic nuclei (AGN) are the main heating source that could offset radiative cooling and prevent 'cooling catastrophes' in clusters of galaxies. There is growing consensus that overall heating and cooling balance may indeed be achieved. This is based on the analysis of statistically significant samples of ICM bubbles (Birzan et al. 2006) as well as other arguments. However, the actual mechanism by means of which the mechanical energy of AGN is delivered to the thermal ICM remains elusive.

The bubbles that supply energy to the ICM are known to be filled with magnetized, relativistic, radio emitting, non-thermal plasma and, thus, the diffusion of cosmic rays (CRs) from magnetic bubbles and their interaction with the ICM is one of the key physical mechanisms that needs to be explored in the context of AGN feedback in clusters. These processes are of high-astrophysical relevance to a number of long-standing problems. If the diffusion rates are relatively high, CR diffusion may explain the absence of strong 'cooling flows', the origin of cluster radio haloes and, as we suggest in this paper, the origin of the excitation of Hα filaments in clusters[1] and the metal distribution in clusters. If, on the other hand, CRs remain largely confined to the bubbles as they rise buoyantly, they may explain the presence of radio relic sources. Such electrons will be protected against Coulomb losses, and are thus able to produce a significant non-thermal Comptonization signature of the CMB.

The effects of CRs diffusion in clusters have been previously studied by, for example, Mathews & Brighenti (2007), who used a

⋆E-mail: mateuszr@umich.edu (MR)

[1] A similar possibility was independently suggested by Sanders & Fabian (2007).

one-dimensional model to put upper limits on the effective diffusivity rate of CRs from AGN-inflated bubbles. These effects were also addressed by Jones, Ryu & Engel (1999) and Tregillis, Jones & Ryu (2004), who performed three-dimensional magnetohydrodynamical (MHD) simulations focusing on a different regime (high-Mach number jets). CR diffusion was also incorporated recently into cosmological structure formation simulations by Miniati (2001) (see also Miniati 2001 for the description of the COSMOCR code) and by Enßlin et al. (2007) and Jubelgas et al. (2006) using the GADGET code.

In this paper, we consider three-dimensional MHD simulations of AGN-inflated bubbles in their buoyant stage. We go beyond previous treatments of this feedback mechanism and include the anisotropy of CR diffusion introduced by magnetic fields in the bubbles. In the next section, we describe the methods employed to simulate anisotropic diffusion. In Section 3, we present our results and in the last section, we discuss the astrophysical consequences of our findings.

2 SIMULATION DETAILS

2.1 The code

The simulations were performed with the PENCIL code (Dobler et al. 2003; Haugen, Brandenburg & Dobler 2003; Brandenburg, Käpylä & Mohammed 2004; Haugen, Brandenburg & Mee 2004). PENCIL is a highly accurate grid code that is sixth order in space and third order in time. It is particularly suited for compressible turbulent MHD flows. Magnetic fields are implemented in terms of a vector potential so the field remains solenoidal throughout the simulation. The code is memory efficient, uses Message-Passing Interface and is highly parallel.

2.2 Initial conditions

The details of the numerical setup pertaining to the thermodynamical state of the cluster atmosphere and magnetic fields were described in detail in (Ruszkowski et al. 2007, hereafter R07). Here, we summarize only the essential points and differences. The distribution of magnetic fields in all runs presented here corresponds to the 'draping case' whereby the characteristic lengthscale of magnetic field fluctuations exceeds the bubble size. The magnetic pressure is much smaller than the gas pressure (typical plasma β parameter is of the order of 20; see R07 for the discussion of this choice). Even though such a magnetic field is formally 'dynamically unimportant', it nevertheless strongly affects the dynamical state of the bubbles by preventing their disruption via the Rayleigh–Taylor and Kelvin–Helmholz instabilities, thus making their morphologies consistent with X-ray observations. Bubbles were initially in total (i.e. CRs and thermal gas) pressure equilibrium with the ambient ICM. For numerical reasons, we chose the CRs pressure to be such that its volume-averaged value was comparable to the thermal pressure. More specifically, the CR pressure fraction $f_{\rm CR}$ was distributed inside the bubble according to $f_{\rm CR}(r) = (1 - f_{\rm gas})\cos(0.5\pi r/r_{\rm b})$, where $f_{\rm gas} = 0.1$ is the pressure fraction due to the thermal gas at the centre of the bubble, $r_{\rm b} = 12.5$ kpc is the bubble radius and r is the distance from the bubble centre. We assumed that the CR contribution to pressure outside the bubble is negligible. The reason we chose CRs pressure distribution that varies as a function of the distance from the bubble centre was numerical. Diffusion problems are very sensitive to sharp spatial gradients and we had to smooth the CRs distribution to avoid numerical problems. The gas inside the cavity was in hydrostatic (pressure) equilibrium in the initial state. That is, the sum of the fractions of the gas and CRs pressures is always equal to unity throughout the computational volume (bubbles included). The bubbles were made buoyantly unstable. At each point within the bubble volume, the gas density was $\rho_{\rm gas} = \rho_{\rm ICM}(1 - f_{\rm CR})/x$ and the gas temperature was $T = T_{\rm ICM}x$, where $x = 10$. The temperature of the ambient ICM was constant and equal to 10 keV (note that high values of temperature lower the effective viscosity of the code as compared to the Braginskii value). A constant value for the ambient temperature also makes it easier to identify the volume occupied by the bubble (i.e. there is no need to introduce a dynamically passive fluid to define the bubble boundaries; we use this fact in the analysis of our simulations below). The reason we opted for a relatively low density and temperature contrasts between the bubble and the ICM was that higher bubble temperatures would have required smaller time-steps to achieve numerical stability of the code.

The resolution of our simulations was 200^3. We used the following code units in this work: code time unit was 3.3×10^6 yr, code length unit was 1 kpc and density unit was 10^{-24} g cm^{-3}. In these units, the diffusivity $K = 32.4(K_0/3 \times 10^{30}$ cm^2 s$^{-1})$ code units, where K_0 denotes the diffusivity in cgs units.

2.3 Cosmic ray diffusion

CRs are incorporated into the code via a two-fluid model. The gas and CR plasmas have adiabatic indices equal to $\gamma = 5/3$ and $\gamma_{\rm cr} = 4/3$, respectively. CRs are coupled to the gas and act on it via their pressure gradient.

Diffusion of relativistic particles in PENCIL takes into account the effects of anisotropy introduced by magnetic fields (diffusion in the direction perpendicular to the field lines is slower than along the field lines).

The standard diffusion equation violates causality by allowing for infinite particle propagation speeds. The diffusion method implemented in the PENCIL code (Snodin et al. 2006) improves on the standard Fick diffusion law and takes into account the requirement that particles should propagate at finite speeds. This is achieved by expanding the Boltzmann equation in the relevant smallness parameter and retaining terms up to second order (see Gombosi et al. 1993 for the discussion of charged particle transport). This treatment is an extension of the method of Hanasz & Lesch (2003), who implemented CR diffusion in the ZEUS code, that included anisotropic diffusion but did not consider departures from the standard diffusion law. The relevant smallness parameter in the expansion of the Boltzmann equation is the Strouhal number $St \equiv (K_\parallel \tau)^{1/2}/l$, where ($K_\parallel$ is the diffusion coefficient along the magnetic field lines, l is the characteristic lengthscale of the initial magnetic structure and τ is the damping time of the non-Fickian contribution to diffusion; Landau & Lifshitz 1987). This approach leads to the generalization of the diffusion equation to the 'telegraph' equation that reduces to the standard diffusion equation in the limit of $St \to 0$ but becomes a wave equation for $St \to \infty$. A non-Fickian diffusion model has also been derived in the context of turbulent diffusion of passive scalars by Blackman & Field (2003) and confirmed in numerical experiments (Brandenburg et al. 2004). More specifically, the standard diffusion equation is replaced with

$$\frac{\partial F_i}{\partial t} = -\hat{K}_{ij}\nabla_j e - \frac{F_i}{\tau}, \quad (1)$$

where F_i is the CR energy flux, e is the CR energy density and $K_{ij} = \tau \hat{K}_{ij}$ is the diffusion tensor given by

$$K_{ij} = K_\perp \delta_{ij} + (K_\parallel - K_\perp)\hat{B}_i \hat{B}_i, \quad (2)$$

where $K_\parallel$ and $K_\perp$ are the CR diffusion coefficients along and perpendicular to the magnetic field, respectively, and $\hat{B}_i = \mathbf{B}|\mathbf{B}|$ is the field-aligned unit vector.

A very rough estimate of the diffusion coefficient can be obtained from a dimensional argument based on the radius of the inner X-ray cavities in the Perseus cluster $r \sim 5r_5$ kpc and the time it takes to inflate the bubble $t \sim 10^7 t_7$ yr Mathews & Brighenti (2007). These values yield $K \lesssim 7.5 \times 10^{29} r_5^2/t_7$ but the estimate is somewhat uncertain. This value is consistent with the theoretical estimates of Enßlin (2003a) $\kappa_\parallel \sim 2 \times 10^{29} E_{10}^{1/3} r_5^{2/3} B_1^{-1/3} \delta^{-1}$ cm^2 s^{-1}, where E_{10} is the energy of radio-emitting electrons in units of 10 GeV, B_1 is the magnetic field in μ Gauss and δ is a parameter of order unity or less that depends on the power spectrum of magnetic field fluctuations and the ratio of particle scattering frequency to gyro-frequency. Assuming that $\tau \sim r/v_A$, where v_A is the Alfvén speed, τ is of order unity in code units for the typical parameters in our simulations. As τ is essentially a free parameter of this model, we adopt this value here. Guided by the above estimates for the diffusion coefficient and the damping time, we estimate the Strouhal number to be $St \sim 0.5(\tau K_\parallel/K)^{1/2}\ (r/r_\mathrm{b})^{-1}$, where $r_\mathrm{b} = 12.5$ is the bubble radius in code units and $K = 32.4$ is the reference diffusivity in code units (in cgs units it is 3×10^{30} cm^2 s^{-1}). The code requires some magnetic diffusivity, η, viscosity, ν, and an isotropic contribution to CR diffusivity, K_iso, to ensure numerical stability. These coefficients can be lowered at the expense of increasing numerical resolution. Except where explicitly stated, in our simulations we adopted $\eta = \nu = K_\mathrm{iso} = 0.07$. As we intend to study the effect of the anisotropy of CR diffusion, we want to keep the ratio of $K_\parallel/K_\mathrm{iso}$ as large as possible. We also want to be conservative in our assessment of the importance of the diffusion and, therefore, consider high values of diffusivity. We stress that for high diffusivities, simulations would not be feasible if not for the fact that the code uses a non-Fickian approach, i.e. effectively limits the CR propagation speed and prevents the time-step from decreasing to unacceptably low values.

3 RESULTS

Fig. 1 shows snapshots from our simulations in the high-diffusivity regime. The first column shows the natural logarithm of thermal gas density in the cluster, while the second and third columns show the logarithm of the CR energy density for two different assumptions about the isotropy of diffusion. The second column corresponds to the case where diffusion in the direction perpendicular to the local magnetic field is suppressed (i.e. $K_\perp = 0$, $K_\parallel = K$), while the last column is for the case where the diffusion coefficients of CR in the direction parallel and perpendicular to the local direction of magnetic field lines are identical. As the density distribution looks quite similar in both the isotopic and the anisotropic cases, we show only the density map for the anisotropic diffusion case. The pressure support at the centre of the bubble comes mostly from CRs ($f_\mathrm{CR} = 0.9$). However, when volume averaged over the entire bubble, it is only at about 10 per cent level. This explains why the bubble does not shrink significantly due to CRs diffusion and why the density distribution in isotropic and anisotropic cases is similar.

The first column in Fig. 1 demonstrates that the 'draping effect' of the magnetic field prevents the disruption of the bubble as it rises buoyantly in the cluster atmosphere. We also note that the magnetic field does not show any signs of decay on the time-scales considered here, either due to numerical effects or to natural relaxation of magnetic fields. While the bubble maintains its integrity, the CRs gradually diffuse out of it. However, this process is not isotropic. In the second column, we see that the spatial distribution of CRs initially tends to follow the distortions in the magnetic field generated by the upwards motion of the bubble (lower panel, second column).

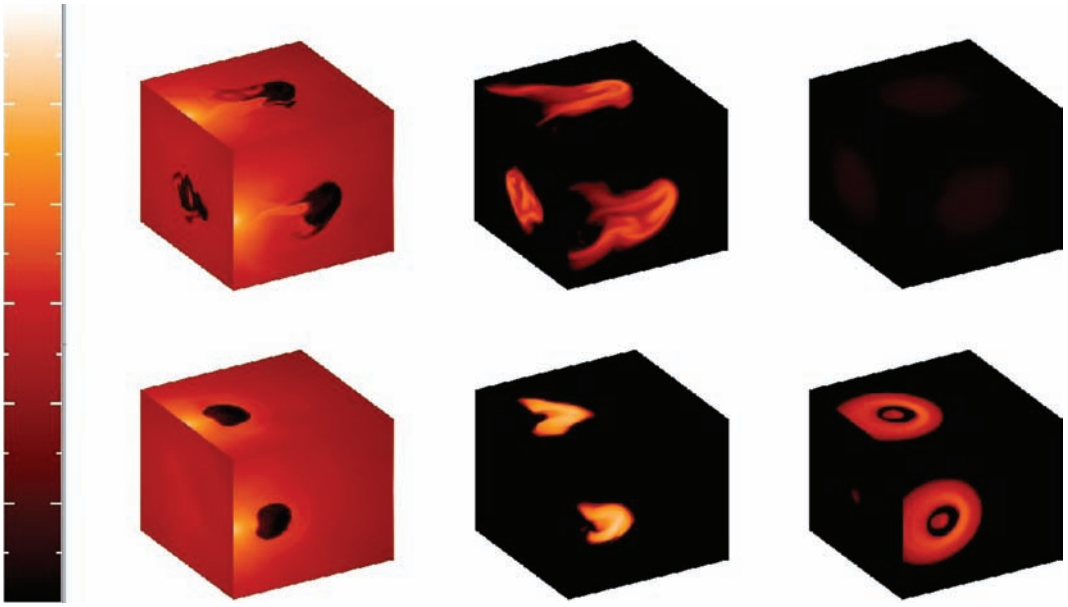

Figure 1. Snapshots of density and CR energy density distributions from three-dimensional PENCIL simulations. The first column shows the natural logarithm of density, while the second and third columns present the logarithm of the energy density of CRs for vanishing diffusion in the direction perpendicular to the local magnetic field ($K_\perp = 0, K_\parallel = K$; middle column) and for the case where the diffusion of CRs in the direction parallel and perpendicular to the local direction of magnetic field lines are identical ($K_\perp = K_\parallel = K$). Lower row corresponds to earlier times $t = 3$, upper to $t = 25$ (one code time unit is 3.3×10^6 yr). In the case of density, the color bar extends from -7.0 to -2.0 in code units. All the remaining columns are for the range $(-3.0, 0.0)$. See the text for more details.

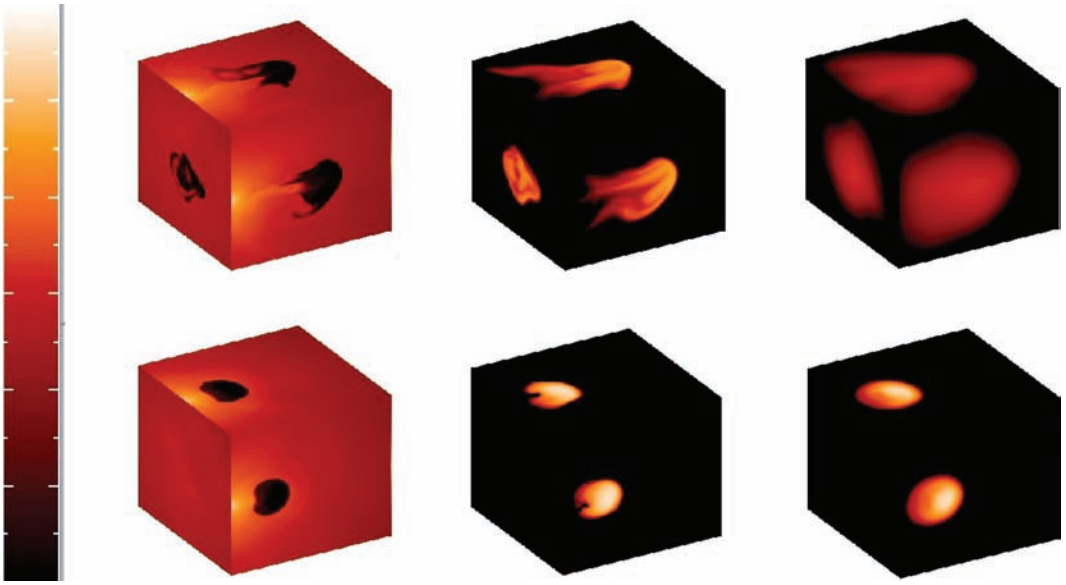

Figure 2. Same as Fig. 1 but for the fiducial value of diffusivity K decreased by a factor of 10.

Magnetic fields and CRs follow the velocity vortex pattern of the rising bubble. At later times (upper row), the magnetic fields inside the bubble 'open up'. This, however, takes place only in the wake of the rising bubble. The working surface of the bubble is efficiently protected from disruption by a thin layer of ordered magnetic fields (see R07 for more detailed discussion of how the field topology changes due to bubble motion). These ordered fields not only prevent instability from developing but also stop CRs from escaping the bubble. On the other hand, magnetic fields stretch out behind the bubble and become approximately parallel to the direction of the motion. CRs can therefore diffuse more easily in the direction of gravity. This effect is clearly seen in the upper row of the second column. In the last column of Fig. 1, we show what happens when diffusion is isotropic (diffusion rates in the directions perpendicular and parallel to the magnetic field lines are identical and equal to the parallel diffusion rate shown in the second column). In this case, the diffusion time is much shorter than the buoyancy time and the pattern of energy density in CRs is markedly different from that corresponding to anisotropic diffusion. In the initial stages of the evolution of CRs energy density, a wave-like pattern is clearly seen – the diffusion signal propagates at finite speed.

Fig. 2 shows the same quantities as Fig. 1 but for the case where the fiducial magnitude of the diffusion coefficient K is reduced by a factor of 10. The viscosity coefficient ν was increased to 0.2 to prevent numerical instabilities for the runs presented in this figure. The arrangement of panels in this figure is the same as in Fig. 1. The density evolution is practically identical. The comparison between the second column with its equivalent in Fig. 1 shows that, as expected, CRs are now better confined to the bubbles (compare the pattern shapes and the CRs intensities). The third column shows that although diffusion is formally isotropic ($K_\perp = K_\parallel$), the diffusion rate is slow enough for the fluid to advect CRs further away from the cluster centre.

In Fig. 3, we quantify the above results in terms of the integrated CR energy normalized to the total initial energy inside the bubbles as a function of time. Dashed lines correspond to the high-diffusivity case (cf. Fig. 1) and solid lines to low-CRs diffusivity (cf. Fig. 2). In each of these two cases, the lower curve corresponds to the isotropic case and the upper one to the case of anisotropic diffusion. These

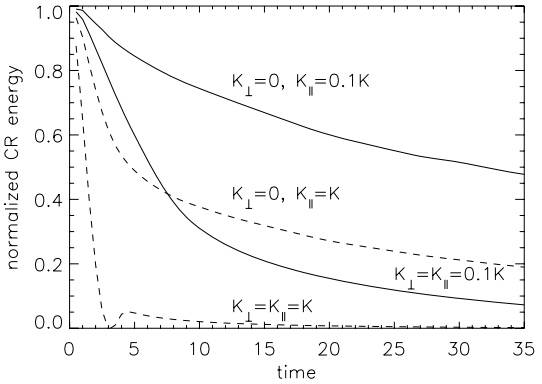

Figure 3. Total energy in CRs inside buoyant bubbles normalized to the total initial energy of CRs as a function of time. Dashed curves are for the high-diffusivity case (cf. Fig. 1) and the solid ones are for low diffusivity (cf. Fig. 2). In each of these two cases, lower curves are for isotropic diffusion and the upper ones for suppressed diffusion in the direction perpendicular to the local orientation of magnetic fields. See the text for more details. All curves correspond to 200^3 runs and $K_{\rm iso} = 0.07$.

curves clearly demonstrate that the anisotropy effects introduced by the topology of the magnetic field are crucial in determining the escape fractions of CRs from AGN bubbles. Anisotropic diffusion can lead to a substantial fraction of CRs being retained inside the bubbles on time-scales of order the buoyancy time. Any diffusion that takes place in such cases is confined to the wake of the bubble. We discuss the implications of these results for the physics of the intracluster medium in the next section.

We also performed a simulation with explicit diffusivity K set to zero. In this case, the only contribution to diffusion comes from isotropic diffusion ($K_{\rm iso}$) that is smaller than the effective diffusion considered in all cases discussed above. In order to perform lower diffusivity simulations, the run had to be performed at higher resolution. The resolution of this simulation was 400^3 with $\nu = 0.2, K = 0$ and $K_{\rm iso} = 0.07$ ($K_{\rm iso}$ is the same as in all cases considered earlier). We found that about 63 per cent of the CRs energy was retained in the bubble in the last output. To further increase the fraction of CRs

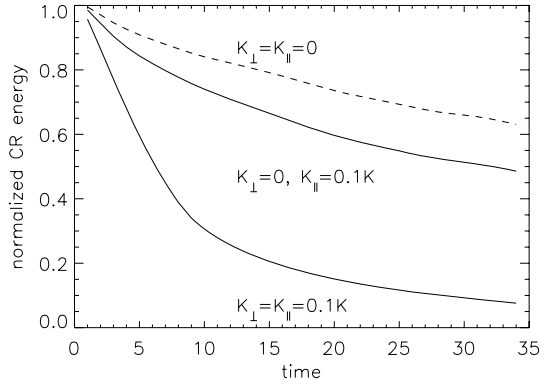

Figure 4. Total energy in CRs inside buoyant bubbles normalized to the total initial energy of CRs as a function of time. All curves correspond to high-resolution run of 400^3 zones and $K_{\rm iso} = 0.07$.

energy retained in the bubble would require lower values of $K_{\rm iso}$. To ensure numerical stability, the 'mesh' Reynolds number $\mathrm{Re}_{\rm mesh} = \upsilon \Delta x / K_{\rm iso}$ (where υ and Δx are a typical velocity and a size of a grid element, respectively) has to be smaller than a certain (small) value. Thus, simulations with lower $K_{\rm iso}$ would require correspondingly higher numerical resolution. We also note that some isotropic contribution to diffusion (i.e. some $K_\perp \ll K_\parallel$) may also be due to anomalous cross-field diffusion (e.g. Enßlin 2003b). Such an effect could be emulated by the contribution of $K_{\rm iso}$ to total diffusion. Thus, non-zero isotropic contribution to diffusion should not be viewed as a purely numerical artefact. To allow for a meaningful comparison of the $K = 0$ case with other cases, we also repeated low-diffusivity isotropic and anisotropic runs discussed in the above at the high resolution of 400^3. First of all, these two additional runs demonstrate that the simulations are numerically convergent. Secondly, in the isotropic case ($K_\parallel = K_\perp = 3.24, K_{\rm iso} = 0.07$), the bubble retains only 7.6 per cent of CRs energy and in the anisotropic case ($K_\parallel = 3.24, K_\perp = 0, K_{\rm iso} = 0.07$) it retains 48 per cent (close to the isotropic limit of 63 per cent). This means that magnetic fields may be quite effective in trapping CRs inside bubbles. However, when diffusion is anisotropic and $K_\parallel$ is larger (see upper dashed curve in Fig. 3), the retained fraction decreases. Note that in all anisotropic diffusion cases, there is no diffusion in the direction of bubble motion (apart from that due to $K_{\rm iso}$), so increasing $K_\parallel$ leads to enhanced CRs escape in the tails of the rising bubbles. In Fig. 4, we show the results of these runs. The dashed curve shows the case for vanishing K, upper solid line is for the anisotropic diffusion and the remaining curve is for isotropic diffusion.

4 ASTROPHYSICAL CONSEQUENCES

The above results have the following astrophysical consequences.

(i) *Radio relics*. Our simulations show that while diffusion out of the bubbles does take place, a significant fraction of the original energy in CRs can be confined to the buoyant bubbles, provided that the perpendicular diffusion coefficient is not too large. Lower values of diffusivity than those considered here would only strengthen this conclusion. If this is the case then CRs can be efficiently screened from Coulomb losses due to their interaction with the ambient medium. Such energetic plasma confined in the bubbles, when subject to passing waves, (either of AGN origin or due to infalling substructure clumps) could be re-energized and lead to detectable radio emission, thus explaining cluster 'radio relic' sources (Enßlin & Brüggen 2002). The fraction of CRs that does escape radio cocoons will pollute the ICM and contribute to the so-called 'radio haloes' Enßlin & Gopal-Krishna (2001).

(ii) *Abundance profiles in clusters of galaxies and entropy injection*. X-ray observations (Schmidt, Fabian & Sanders 2002; Böhringer et al. 2004; De Grandi et al. 2004; *in Virgo, Perseus, Centaurus* and *Abell 1795 clusters*) reveal that clusters without cool cores show a spatially uniform distribution of metals while cooling flow clusters reveal strong centrally peaked metallicity profiles. However, the observed metallicity profiles appear much broader than the stellar light distribution of the brightest cluster galaxies (BCGs). One possible solution to this puzzle is that AGN help to uplift the gas enriched with metals (e.g. Brüggen 2002; Roediger et al. 2007). In the absence of any microscopic energy transfer between the interior of the bubble filled with relativistic plasma and the displaced metal-enriched thermal gas, the latter will tend to sink back towards the cluster centre. This problem is closely related to the problem of the development of hydrodynamical instabilities on the bubble-ICM interface. In the absence of any mechanism to suppress such instabilities (such as viscosity or magnetic fields), the rising bubble will be quickly shredded and the non-thermal bubble material will mix with the ICM, adding entropy to the metal-enriched gas and preventing it from sinking towards the cluster centre. This is what happens in pure hydrodynamical simulations. In a realistic situation, magnetic fields may help to prevent such instabilities and the entropy gain of the metal-enriched gas must have a different origin. Here, we suggest that the diffusion of CRs out of the bubbles and their subsequent thermalization may provide the necessary energy injection.

Depending on the energy of radiating electrons and the density of the ICM, either Coulomb interaction of CRs electrons with the ICM ($t^{\rm Coul}_{\rm cool} \sim 2 \times 10^8 \gamma_2 n_{-2}^{-1}$ yr) or synchrotron/inverse Compton energy losses will dominate [$t^{\rm IC}_{\rm cool} \sim 2 \times 10^8 \gamma_4^{-1} (1 + u_{\rm B}/u_{\rm IC})$ yr], where n_{-2} is the electron density in units of 10^{-2} cm^{-3}, $\gamma_{2,4}$ is the relativistic γ factor in units of 10^2 and 10^4, respectively, and $u_{\rm B,\,IC}$ are the energy densities in magnetic fields and CMB photons, respectively.

We assume that most of the CR energy is carried by protons. In this case, CRs cool (efficiently) via Coulomb interactions with a medium if they are non-relativistic and cool (inefficiently) via hadronic interactions if they are relativistic. In the latter case, CRs energy interact with the ICM inelastically and produce pions. The decay of pions results in the production of γ-rays, neutrinos as well as secondary electrons that can also heat the ICM via Coulomb interactions. When the CR momentum injection spectrum has a power-law dependence with a lower momentum cut-off $\ll m_{\rm p}c$, then a steady state population emerges with a peak in the momentum spectrum at $\sim m_{\rm p}c$ (see fig. 6 in Enßlin et al. 2007). Note also that for this momentum most of the losses are due to Coulomb interactions (see fig. 4 in Enßlin et al. 2007). Thus, after a short initial period (one cooling time at $\sim$1 GeV), the cooling time around $\sim m_{\rm p}c$ is the typical energy transfer time $\sim 10^8 (n/0.05\ \mathrm{cm}^{-3})^{-1}\ (p/m_{\rm p}c)$ yr, where n is the number density in the ICM. This time-scale is roughly comparable to the bubble dynamical time-scale.

An alternative mechanism to tap the energy of CRs is the damping of MHD waves excited by CRs streaming along the magnetic field lines (Loewenstein, Zweibel & Begelman 1991 and references therein, Guo & OH 2007). The lengthscale over which the streaming CRs lose their energy is equal to CRs pressure scaleheight. Thus, if there is a an open field line with a strong CRs pressure gradient, CRs may efficiently lose their energy and heat the gas. As argued by R07, such B-field configurations occur in the wakes of the bubbles where fields tend to open up and align with the bubble wake.

Thus, the thermalization of CRs may then preferentially increase the entropy of the metal-enriched material being pulled up in the cluster atmosphere by buoyantly rising bubbles. This is because CRs tend to preferentially diffuse in the direction opposite to their motion, i.e. their thermalization may mostly take place in the metal-enriched ICM dragged behind the bubbles (at least for the magnetic field parameters considered here). One can estimate that the change of ICM entropy per outburst may be approximated as $\Delta K/K = 0.66\gamma/(\gamma - 1)f_{\rm diff}V_{\rm b}/V_{\rm ICM}$, where $K = kT/n^{2/3}$, γ is the adiabatic index of the gas inside the bubbles, $f_{\rm diff}$ is the fraction of CRs energy that escaped the bubble and $V_{\rm b}/V_{\rm ICM}$ is the ratio of the bubble volume to the volume of the ICM over which CRs have been thermalized, and n and T are the particle number density and temperature of the ICM. As argued above the thermalization time-scale due of CRs in the 'cold' ICM gas can be comparable to $\sim 10^8$ yr. This is of the order of the bubble rise time-scale (see Figs 1 and 2). If the CRs diffuse and thermalize in the wake of the bubble then $V_{\rm b}/V_{\rm ICM}$ can be roughly comparable to unity. Thus, we estimate that a one (or a few) AGN outbursts could easily double the entropy of the ICM in the vicinity of bubbles. Such entropy change would clearly suffice to displace and lift the metal-enriched gas. We speculate that the metalicity dips observed in the very centres of the Perseus (Sanders & Fabian 2007) and Centaurus (Sanders & Fabian 2006) clusters may be due to the above effects.

(iii) *Excitation of Hα line in the filaments trailing behind bubbles*. Emission-line nebulae are commonly found surrounding massive galaxies in the centres of cool cluster cores (Crawford et al. 1999). The best examples of extended Hα-emitting filaments pointing from the cluster centre to the buoyant bubbles are those in the Perseus cluster (Hatch et al. 2006). Several mechanism have been proposed (and ruled out) to explain the excitation mechanism of this line. One possibility is that these nebulae are excited by stellar ultraviolet (UV), but there is no spatial correlation between the filaments and stellar clusters (Hatch et al. 2006). Another mechanism could be excitation by X-rays from the ICM but the filaments are up to a hundred times less luminous in X-rays than in the UV (Fabian et al. 2003b). Finally, it has been proposed that heat conduction from the ICM to the colder filaments could provide line excitation (Donahue et al. 2000). However, thermal conductivity would also lead to the evaporation of these filaments (Nipoti & Binney 2004). Here, we suggest the possibility that CRs, preferentially diffusing along the field lines trailing behind the rising bubbles, could provide the excitation mechanism for the filaments that are also located in the bubble wakes. We note that the same magnetic fields that act like 'wires' conducting CRs could also prevent the filaments from evaporating via thermal conductivity by locally suppressing it. As a side note we add that while the ICM may be viscous, the laminar appearance of the filaments does not necessarily imply that the flow is viscous. The ordered and amplified magnetic fields trailing behind the bubble may prevent the destruction of the filaments by turbulent motions.

(iv) *γ-ray signatures*. It has recently been proposed that extended radio features of radio galaxies (Sambruna et al. 2007; in case of Fornax A) and the interaction of CRs from AGN cavities with the ICM (Hinton, Domainko & Pope 2007; Hydra A) could be detectable with the Gamma-ray Large Area Space Telescope. Moreover, it has been pointed out that the interaction of such CRs with the ICM could lead to significant annihilation line emission (Furlanetto & Loeb 2002; Griffiths 2005). We point out that our simulations add more weight to this idea and that a preferential diffusion of CRs in the wakes of rising bubbles could potentially lead to observable γ-ray signatures.

We also note that these results emphasize the role of non-ideal hydrodynamical effects in the studies of AGN feedback in general. While we argued here that CR diffusivity may be one of the key effects that needs to be included, other transport process such as conduction (Ruszkowski & Begelman 2002; Brüggen, Ruszkowski & Hallman 2005; Fabian et al. 2005) or viscosity (Fabian et al. 2003a; Ruszkowski, Brüggen & Begelman 2004a,b; Reynolds et al. 2005; Sijacki & Springel 2006) may also play an important role. Finally, if the 'pollution' of the intracluster medium by CRs diffusing out of AGN bubbles is significant, then other mechanisms such as the generalization of the magnetothermal instability (Balbus 2004; Parrish & Stone 2005) by Chandran (2005) may also play a role. We note that recent X-ray observations with *Chandra* and *XMM–Newton* show evidence for non-thermal particle populations in the ICM (Sanders & Fabian 2006; Werner et al. 2007).

ACKNOWLEDGMENTS

We thank the referee for very useful suggestions. MR thanks Andrew Snodin for discussions. All simulations were performed on the Columbia supercomputer at NASA Ames centre. It is MR's pleasure to thank the staff of NAS, and especially Johnny Chang and Art Lazanoff for their highly professional help. The PENCIL Code community is thanked for making the code publicly available. The main code website is located at http://www.nordita.dk/software/pencil-code/. MB acknowledges support by the Deutsche Forschungsgemeinschaft grant BR 2026/3 within the Priority Programme 'Witnesses of Cosmic History', and MCB acknowledges partial support under National Science Foundation grant AST-0307502.

REFERENCES

Balbus S. A., 2004, ApJ, 616, 857
Birzan L., McNamara B. R., Carilli C. L., Nulsen P. E. J., Wise M. W., 2006, preprint (arXiv:astro-ph/0612393)
Blackman E. G., Field G. B., 2003, Phys. Fluids, 15, L73
Blanton E. L., Sarazin C. L., McNamara B. R., 2003, ApJ, 585, 227
Böhringer H., Matsushita K., Churazov E., Finoguenov A., Ikebe Y., 2004, A&A, 416, L21
Brandenburg A., Käpylä P. J., Mohammed A., 2004, Phys. Fluids, 16, 1020
Brüggen M., 2002, ApJ, 571, L13
Brüggen M., Ruszkowski M., Hallman E., 2005, ApJ, 630, 740
Chandran B. D. G., 2005, ApJ, 632, 809
Crawford C. S., Allen S. W., Ebeling H., Edge A. C., Fabian A. C., 1999, MNRAS, 306, 857
De Grandi S., Ettori S., Longhetti M., Molendi S., 2004, A&A, 419, 7
Dobler W., Haugen N. E., Yousef T. A., Brandenburg A., 2003, Phys. Rev. E, 68, 026304
Donahue M., Mack J., Voit G. M., Sparks W., Elston R., Maloney P. R., 2000, ApJ, 545, 670
Enßlin T. A., 2003a, A&A, 401, 499
Enßlin T. A., 2003b, A&A, 399, 409
Enßlin T. A., Gopal-Krishna, 2001, A&A, 366, 26
Enßlin T. A., Brüggen M., 2002, MNRAS, 331, 1011
Enßlin T. A., Pfrommer C., Springel V., Jubelgas M., 2007, A&A, 473, 41
Fabian A. C., Sanders J. S., Allen S. W., Crawford C. S., Iwasawa K., Johnstone R. M., Schmidt R. W., Taylor G. B., 2003a, MNRAS, 344, L43
Fabian A. C., Sanders J. S., Crawford C. S., Conselice C. J., Gallagher J. S., Wyse R. F. G., 2003b, MNRAS, 344, L48
Fabian A. C., Reynolds C. S., Taylor G. B., Dunn R. J. H., 2005, MNRAS, 363, 891

Fabian A. C., Sanders J. S., Taylor G. B., Allen S. W., Crawford C. S., Johnstone R. M., Iwasawa K., 2006, MNRAS, 366, 417
Furlanetto S. R., Loeb A., 2002, ApJ, 572, 796
Gombosi T. I., Jokipii J. R., Kota J., Lorencz K., Williams L. L., 1993, ApJ, 403, 377
Griffiths R. E., 2005, Exp. Astron., 20, 23
Guo F., OH S. P., 2007, MNRAS, prepress (arXiv:0706.1274)
Hanasz M., Lesch H., 2003, A&A, 412, 331
Hatch N. A., Crawford C. S., Johnstone R. M., Fabian A. C., 2006, MNRAS, 367, 433
Haugen N. E. L., Brandenburg A., Dobler W., 2003, ApJ, 597, L141
Haugen N. E. L., Brandenburg A., Mee A. J., 2004, MNRAS, 353, 947
Hinton J. A., Domainko W., Pope E. C. D., 2007, MNRAS, 382, 466
Jones T. W., Ryu D., Engel A., 1999, ApJ, 512, 105
Jubelgas M., Springel V., Ensslin T. A., Pfrommer C., 2006, preprint (arXiv:astro-ph/0603485)
Landau L. D., Lifshitz F. M., 1987, Fluid Mechanics, 2nd edn. Pergamon Press, Oxford
Loewenstein M., Zweibel E. G., Begelman M. C., 1991, ApJ, 377, 392
Mathews W. G., Brighenti F., 2007, ApJ, 660, 1137
Miniati F., 2001, Comput. Phys. Commun., 141, 17
Nipoti C., Binney J., 2004, MNRAS, 349, 1509
Parrish I. J., Stone J. M., 2005, ApJ, 633, 334
Reynolds C. S., McKernan B., Fabian A. C., Stone J. M., Vernaleo J. C., 2005, MNRAS, 357, 242
Roediger E., Brüggen M., Rebusco P., Böhringer H., Churazov E., 2007, MNRAS, 375, 15
Ruszkowski M., Begelman M. C., 2002, ApJ, 581, 223
Ruszkowski M., Brüggen M., Begelman M. C., 2004a, ApJ, 615, 675
Ruszkowski M., Brüggen M., Begelman M. C., 2004b, ApJ, 611, 158
Ruszkowski M., Enßlin T. A., Brüggen M., Heinz S., Pfrommer C., 2007, MNRAS, 378, 662 (R07)
Sanders J. S., Fabian A. C., 2006, MNRAS, 371, 1483
Sanders J., Fabian A. C., 2007, MNRAS, 381, 1381
Sambruna R. M., Georganopoulos M., Davis D., Cillis A., 2007, preprint (arXiv:0704.1112)
Schmidt R. W., Fabian A. C., Sanders J. S., 2002, MNRAS, 337, 71
Sijacki D., Springel V., 2006, MNRAS, 371, 1025
Snodin A. P., Brandenburg A., Mee A. J., Shukurov A., 2006, MNRAS, 373, 643
Tregillis I. L., Jones T. W., Ryu D., 2004, ApJ, 601, 778
Werner N., Kaastra J. S., Takei Y., Lieu R., Vink J., Tamura T., 2007, A&A, 468, 849

This paper has been typeset from a TEX/LATEX file prepared by the author.